

PPPL-2234

PPPL-2234

UC20-G

② 7-1278-5
I-22896

②E

THREE-DIMENSIONAL STELLARATOR EQUILIBRIUM
AS AN OHMIC STEADY STATE

By

W. Park, D.A. Monticello, H. Strauss, and J. Manickam

JULY 1985

MASTER

PLASMA
PHYSICS
LABORATORY



PRINCETON UNIVERSITY
PRINCETON, NEW JERSEY

PREPARED FOR THE U.S. DEPARTMENT OF ENERGY,
UNDER CONTRACT DE-AC02-76-CFO-3013

DISTRIBUTION OF THIS DOCUMENT IS UNLIMITED

THREE-DIMENSIONAL STELLARATOR EQUILIBRIUM
AS AN OHMIC STEADY STATE

W. Park, D.A. Monticello, H. Strauss[†], and J. Manickam

Plasma Physics Laboratory, Princeton University

P. O. Box 451, Princeton, NJ 08544

PPPL--2234

DE85 017683

ABSTRACT

A stable three-dimensional stellarator equilibrium can be obtained numerically by a time-dependent relaxation method using small values of dissipation. The final state is an ohmic steady state which approaches an ohmic equilibrium in the limit of small dissipation coefficients. We describe a method to speed up the relaxation process and a method to implement the $\vec{B} \cdot \nabla p = 0$ condition. These methods are applied to obtain three-dimensional heliac equilibria using the reduced heliac equations.

DISCLAIMER

This report was prepared as an account of work sponsored by an agency of the United States Government. Neither the United States Government nor any agency thereof, nor any of their employees, makes any warranty, express or implied, or assumes any legal liability or responsibility for the accuracy, completeness, or usefulness of any information, apparatus, product, or process disclosed, or represents that its use would not infringe privately owned rights. Reference herein to any specific commercial product, process, or service by trade name, trademark, manufacturer, or otherwise does not necessarily constitute or imply its endorsement, recommendation, or favoring by the United States Government or any agency thereof. The views and opinions of authors expressed herein do not necessarily state or reflect those of the United States Government or any agency thereof.

[†]Permanent address: Courant Institute for Mathematical Sciences, New York University, New York, NY 10012

DISTRIBUTION OF THIS DOCUMENT IS UNLIMITED

ep

I. INTRODUCTION

In obtaining three-dimensional (3-D) equilibria numerically, one encounters some basic difficulties. For example, the final magnetic topology is not known beforehand, because magnetic islands and stochastic regions may develop. To make the calculation more tractable, existing 3-D equilibrium codes¹⁻³ either have assumed good flux surfaces or have taken a nonzero field-line-averaged current. One way to determine 3-D equilibria and not make any nonphysical assumptions is to use an initial value approach. Stable 3-D stellarator equilibria will have a nearby ohmic steady state. This ohmic state can be, in principle, found from a nonequilibrium initial state by a time-dependent relaxation process using small values of resistivity η and viscosity μ . However, a straightforward application of this method requires a large amount of computing time because dissipation coefficients have to be quite small for the final ohmic state to be equivalent to the equilibrium state. In Sec. II, a method to speed up the convergence process will be described.

Another major obstacle in determining 3-D equilibria is the implementation of the condition, $\vec{B} \cdot \nabla p = 0$, which requires the pressure to conform to magnetic island shapes and to be constant in stochastic regions. An efficient method to implement this condition is also described in Sec. II.

Finally in Sec. III, we apply our method to obtain heliac⁴ equilibria, using the reduced high beta heliac equations.⁵

II. METHODS

A magnetohydrodynamic (MHD) equilibrium satisfies the force balance condition

$$\vec{J} \times \vec{B} = \nabla p \quad . \quad (1)$$

In addition, a stellarator (ohmically relaxed) equilibrium satisfies the zero field-line-averaged current condition

$$\langle \eta \vec{J} \cdot \vec{B} \rangle = 0 \quad . \quad (2)$$

Here $\langle f \rangle$ is defined as $(\int (f/B) dl) / (\int (1/B) dl)$, where dl is along the magnetic field \vec{B} . When good flux surfaces exist, the condition (2) was shown to be equivalent to the $dI = 0$ condition in Ref. 6, where dI is the net toroidal current between two flux surfaces.

In principle, these equilibria can be obtained to arbitrarily high accuracy by integrating the following MHD equations using small resistivity η and viscosity μ .

$$\rho \frac{\partial \vec{v}}{\partial t} = -\rho \vec{v} \cdot \nabla \vec{v} - \nabla p + \vec{J} \times \vec{B} + \mu \nabla^2 \vec{v} \quad , \quad (3)$$

$$\frac{\partial \vec{B}}{\partial t} = \text{curl} (\vec{v} \times \vec{B} - \eta \vec{J}) \quad , \quad (4)$$

$$\frac{\partial \rho}{\partial t} = -\text{div}(\rho \vec{v}) + S_\rho \quad , \quad (5)$$

$$\frac{\partial p}{\partial t} = -\vec{v} \cdot \nabla p - \gamma p \text{div} \vec{v} + \rho \vec{v} \cdot \left\{ \kappa \cdot \nabla \left(\frac{p}{\rho} \right) \right\} + S_p \quad . \quad (6)$$

Here rationalized emu units are used, and the density source S_ρ and pressure source S_p are necessary to balance the diffusion losses.

The zero field-line-averaged current condition (2) is a direct

consequence of Eq. (4), which gives

$$\vec{v} \times \vec{B} - \eta \vec{J} = -\nabla \chi = -\vec{E}$$

for a steady state. The potential χ is single valued for stellarators for which the applied loop voltage is zero. Thus

$$\langle \eta \vec{J} \cdot \vec{B} \rangle = \langle \nabla \chi \cdot \vec{B} \rangle = 0$$

In this picture, a stellarator equilibrium is a dynamo system supported by the pressure source S_p .

As a first step for simplification of Eqs. (3)-(6), we set $\rho = 1$ and drop Eq. (5) by assuming an appropriate density source S_ρ . Next we examine Eq. (6) which gives the $\vec{B} \cdot \nabla p = 0$ condition.

A. $\vec{B} \cdot \nabla p = 0$ condition

The large parallel thermal conductivity κ_{\parallel} ($\kappa_{\parallel} \gg \kappa_{\perp}$) in Eq. (6) will give the constant pressure along the field line condition ($\vec{B} \cdot \nabla p = 0$), as required by Eq. (1). The pressure will be constant in a stochastic region and will conform to magnetic island shapes. However, to our knowledge there is no satisfactory numerical method for 3-D problems to handle the large disparity between the parallel and perpendicular conductivity. Thus, we replace Eq. (6) with the following artificial sound equations with fixed \vec{B} ,

$$\partial p / \partial t = \vec{B} \cdot \nabla v_a$$

$$\partial v_a / \partial t = \vec{B} \cdot \nabla p$$

(7)

The artificial velocity v_a is analogous to the parallel velocity v_{\parallel} . It is easy to show that this system of equations has a conserved energy $E_a = 1/2 \int (p^2 + v_a^2) d\tau$, and that the flux-tube-averaged pressure $\langle p \rangle$ is conserved. The equilibrium state of Eq. (7) satisfies the $\vec{B} \cdot \nabla p = 0$ condition.

An efficient way to find an equilibrium of any energy conserving system is the method of "kinetic energy quenching".⁸ During the time integration of Eqs. (7), the kinetic energy $K = 1/2 \int v_a^2 d\tau$ is monitored. When K reaches a maximum and starts to decrease, we set $v_a = 0$, thereby removing the kinetic energy. Note that for a system of a single degree of freedom, one such operation will give the exact equilibrium. For the present system, several such operations in sequence are usually necessary. Since no dissipation coefficient is used in this method, the equilibrium is found in an ideal time scale given by \vec{B} .

B. A method to speed up the convergence.

In the method described thus far, we alternate the " $\vec{B} \cdot \nabla p = 0$ process" with fixed \vec{B} described in Sec. IIA and the "relaxation process" given by the following equations with fixed p .

$$\frac{\partial \vec{v}}{\partial t} = - \vec{v} \cdot \nabla \vec{v} - \nabla p + \vec{\kappa} \vec{B} + \mu \nabla^2 \vec{v} ,$$

$$\frac{\partial \vec{B}}{\partial t} = \text{curl} (\vec{\kappa} \vec{B} - \eta \vec{j}) . \quad (8)$$

The relaxation process takes a very long computing time because both the resistivity η and viscosity μ have to be quite small for the final ohmic state to be equivalent to the equilibrium state. To speed up the relaxation

process, we drop the convection term, $\vec{v} \cdot \nabla \vec{v}$, in Eqs. (8). (This does not change the equilibrium nor the linear stability conditions.)

Then, the final ohmic steady state does not depend on η and μ separately but depend only on the product $(\eta\mu)$. This can be seen easily by noting that changes of $\eta \rightarrow \alpha\eta$ and $\mu \rightarrow \mu/\alpha$ changes \vec{v} to $\alpha\vec{v}$ but leaves p and \vec{B} the same, in a steady state. Since only the product $(\eta\mu)$ must be small, we can use a larger η to speed up the relaxation, while using a small enough μ so that the product $(\eta\mu)$ is small. In this formulation, the damping of kinetic energy occurs not due to the viscosity but due to resistive Alfvén modes of finite resistivity. Of course, the value of η cannot be too large because the ideal Alfvén wave effect is necessary in the relaxation to the force balance. The present method of dropping the convection term can be used in any situation where an ohmic steady state with vanishing zeroth order flow (i.e., $\vec{v} \rightarrow 0$ as $\eta \rightarrow 0$) is desired.

Summarizing our methods, we alternate the $\vec{B} \cdot \nabla p = 0$ process with fixed \vec{B} described in Sec. IIA and the relaxation process given by

$$\frac{\partial \vec{v}}{\partial t} = -\nabla p + \vec{v} \times \vec{B} + \mu \nabla^2 \vec{v} \quad , \quad (9)$$

$$\frac{\partial \vec{B}}{\partial t} = \text{curl} (\vec{v} \times \vec{B} - \eta \vec{J}) \quad ,$$

with fixed p , until a 3-D ohmic state is obtained. The dissipation coefficients are chosen such that $\eta \gg \mu$ to speed up the relaxation process while keeping the product $(\eta\mu)$ small so that the ohmic steady state obtained is equivalent to a stable 3-D stellarator equilibrium.

III. HELIAC EQUILIBRIA

The methods described in the previous section are incorporated in a numerical code HIBS to find 3-D heliac equilibria using the reduced heliac equations.⁵ Heliac⁴ is a helical axis stellarator with comparable amounts of toroidal and helical shifts, producing intrinsically three-dimensional equilibria.

A. The reduced heliac equations

The reduced equation describing heliacs with $\beta \sim 1$ are

$$\frac{\partial \nabla^2 u}{\partial t} = - \hat{v} \cdot \hat{v} \nabla^2 u + (1-p) \hat{B}^0 \cdot \nabla \nabla^2 \psi + \nabla p \times \hat{k} \cdot \hat{\phi} + \mu \nabla^2 \nabla^2 u, \quad (10)$$

$$\frac{\partial \psi}{\partial t} = \hat{B}^0 \cdot \nabla u + \eta \nabla^2 \psi, \quad (11)$$

$$\frac{dp}{dt} = \nabla \cdot (\kappa \nabla p), \quad (12)$$

where $\hat{v} = \nabla u \times \hat{\phi}$,

$$\hat{B} = B \hat{b} = B (\hat{B}^0 / B_0) = \frac{B}{B_0} \hat{B}^0 = \sqrt{1-p} \hat{B}^0,$$

$$\hat{B}^0 = \nabla \psi \times \hat{\phi} + B_0 \hat{\phi},$$

$$\hat{k} = \nabla \left[-\frac{x}{g} + \frac{1}{2} |\nabla \psi|^2 \right] - (\nabla^2 \psi) \nabla \psi + \nabla \frac{\partial \psi}{\partial \phi} \times \hat{\phi},$$

and p is the local β value, $p = \text{pressure} / (B_0^2 / 2)$. Here, (r, θ, ϕ) are the usual toroidal coordinates, B_0 is the vacuum toroidal field strength, and constant density $\rho = 1$ is used. Rationalized emu units are used as before. To derive

these equations, the ratio $\delta = a/(l/2\pi)$ is assumed to be small, where a is the machine minor radius and l the length of one helical period. The orderings taken are rotational transform per helical period $\alpha \sim 1$, and the total number of helical periods $N \sim \delta^{-1}$.

The free parameter $g = N\delta$ is the ratio between the helical curvature $\sim \delta^2/a$ and toroidal curvature $R_0^{-1} \sim \delta/(aN)$ of magnetic fields, thus determining the ratio between helical and toroidal shifts.

B. Methods for heliac equilibria

To apply the $\vec{B} \cdot \nabla p = 0$ process, the pressure Eq. (12) is replaced by the following artificial sound equations and solved as described in Sec. IIA.

$$\begin{aligned} \frac{\partial p}{\partial t} &= \vec{B}^0 \cdot \nabla v_a \quad , \\ \frac{\partial v_a}{\partial t} &= \vec{B}^0 \cdot \nabla p \quad , \end{aligned} \tag{13}$$

where

$$\vec{B}^0 = B_0 \hat{b} = \nabla\psi \times \hat{\phi} + B_0 \hat{\phi} \quad .$$

Before we state the equations analogous to Eq. (9), we must take account of the fact that the central conductor of the heliac is inside our computational domain. We treat this conductor as if it is a rigid ion beam with fixed current that allows plasma to go through it. This can be accomplished⁷ by modifying the MHD equations. Using the beam current density

\vec{j}_b

$$\frac{\partial \vec{v}}{\partial t} = \dots + (\vec{J} - \vec{J}_b) \times \vec{B} ,$$

$$\frac{\partial \vec{B}}{\partial t} = \text{curl} \{ \dots + \eta (\vec{J} - \vec{J}_b) \} .$$

Incorporating this procedure and the method of Sec. IIB, the relaxation process uses the equations,

$$\partial \nabla^2 u / \partial t = (1-p) \vec{B}^0 \cdot \nabla (\nabla^2 \psi + J_{b\phi}) + \nabla p \times \hat{k} \cdot \hat{z} + \mu \nabla^2 \nabla^2 u , \quad (14)$$

$$\frac{\partial \psi}{\partial t} = \vec{B}^0 \cdot \nabla u + \eta (\nabla^2 \psi + J_{b\phi}) .$$

This system of equations conserves energy E with $\eta = \mu = 0$, if $dp/dt = 0$ is used for the pressure, where

$$E = \int d\tau \left[\frac{1}{2} |\nabla u|^2 + \frac{1}{2} (1-p) |\nabla \psi - \nabla \psi_b|^2 - (x/g - \frac{1}{2} |\nabla \psi_b|^2) p \right] ,$$

and

$$\nabla^2 \psi_b = - J_{b\phi} .$$

The fact that fixed pressure is used in the relaxation process represents the pressure source which drives the dynamo system and sustains the heliac equilibrium.

C. Numerical methods

The numerical code HIBS is the stellarator mode of the HIB code.⁸ The r direction dependence is represented in a finite difference scheme while (θ, ϕ)

space is represented in a (m,n) Fourier space. All the dissipation terms are solved implicitly while other terms are solved explicitly. Very large resistivity and viscosity values are used in the vacuum region to further speed up the convergence. This does not affect the final solution because there is no velocity or current in that region in the final ohmic steady state.

One of the most cumbersome aspects of 3-D calculations in Fourier space is the management of harmonics. To alleviate this problem, the HIB code has been designed to determine automatically the necessary harmonics and add or eliminate different (m,n) harmonics as the harmonics requirement changes during the computation.

D. Results

As an application of the methods described in the previous sections, we here study heliac equilibria with a machine aspect ratio $A = 5$ and the total number of helical periods $N = 5$. Figure 1 shows pressure contours of an equilibrium with the peak beta $\beta_M = 10\%$. Large $m = 2$ magnetic islands have formed because the magnetic surface with rotational transform per helical period $\kappa = 0.5$ lies inside the plasma. Figure 1(a) shows the poloidal crosssection at $\phi = 0$ and Fig. 1(b) at $\phi = \pi$ where ϕ is the toroidal anglelike variable of one helical period.

We next change the external parameters so that the $\kappa = 0.5$ surface moves out of the plasma, as shown in the κ profile, Fig. 2. Note that a low mode number resonance with $\kappa = n/m$ does not occur inside the plasma. The small rise of κ inside the plasma is due to the equilibrium plasma pressure which we kept the same as in the previous case with $\beta_M = 10\%$.

Figures 3(a), (b), and (c) are the pressure contours of this equilibrium

at various ϕ angles. The major axis is to the left in each picture. The magnetic axis at zero beta was at $r = 0.5$. The toroidal shift is about 15% of the plasma size and the helical shift about 5%. The boundary of the plasma also changes self-consistently forming a free boundary equilibrium. Figure 3(c) shows the puncture plot of magnetic fields. Two $m = 2$ islands lie just outside of the plasma and the region around the main separatrix became stochastic.

Figure 4 shows current density contours. In Figs. 4(a) and (b), we can see that the zero field-line-averaged current condition, $\langle \eta \mathbf{J} \cdot \mathbf{B} \rangle = 0$, is satisfied. In Figure 4(c), the current induced by the toroidal shift and the current induced by the helical shift interfere destructively and the resulting current density is small but complicated. It is interesting to note that the destructive interference occurs where the toroidal and helical shifts are in the same directions. Figure 4(d) shows the central conductor current.

A drastic deformation of the plasma occurred as shown in Fig. 5, as we increased the pressure of the previous equilibrium to $\beta_H = 12\%$ while keeping all the other parameters fixed. The pressure contours, Fig. 5, look similar to a typical nonlinear evolution of low n ballooning modes,⁹ indicating that the plasma may become unstable to ballooning modes. The subsequent evolution requires a long computing time due to its complex structure, and will be studied in the future.

IV. SUMMARY

We have described a procedure to obtain three-dimensional stellarator equilibria by a time-dependent relaxation process. The equilibria thus obtained are stable free-boundary equilibria which satisfy the zero field-line-averaged current condition. The main techniques employed in the

procedure are a method to speed up the relaxation process described in Sec. IIB and a method to satisfy the $\vec{E} \cdot \nabla p = 0$ condition described in Sec. IIA.

In Sec. III, heliac equilibria are obtained using the above methods. In this application, we have used the high- β reduced heliac equations. An equilibrium with good flux surfaces with $\beta_M = 10\%$ is obtained for the given machine parameters. When β_M is increased to 12%, a sudden onset of a ballooning-like instability occurred.

ACKNOWLEDGMENTS

We wish to thank Drs. A.H. Boozer, R.A. Ellis, J.L. Johnson, and R.M. Kulsrud for helpful discussions.

This work was supported by U.S. DoE Contract No. DE-AC02-76-CHO-3073.

REFERENCES

- ¹F. Bauer, O. Betancourt, and P. Garabedian, A Computational Method in Plasma Physics (Springer, New York, 1978).
- ²R. Chodura and A. Schlüter, *J. Comput. Phys.* 41, 68 (1981).
- ³T.C. Hender, B.A. Carreras, and V.E. Lynch, *Bull. Am. Phys. Soc.* 27, 1020 (1982).
- ⁴H.P. Furth, J. Killeen, M.N. Rosenbluth, and B. Coppi, in Plasma Physics and Controlled Nuclear Fusion Research (IAEA, Vienna, 1966), Vol. I, p. 103.
- ⁵H.R. Strauss, D.A. Monticello, and W. Park, *Nucl. Fusion* (submitted for publication).
- ⁶M.D. Kruskal and R.M. Kulsrud, *Phys. Fluids* 1, 265 (1958).
- ⁷J.L. Johnson, R.M. Kulsrud, and K.E. Weimer, *Plasma Phys.* 11, 463 (1969).
- ⁸W. Park, D.A. Monticello, and R.B. White, *Bull. Am. Phys. Soc.* 23, 779 (1978); H.R. Strauss, W. Park, D.A. Monticello, R.B. White, S.C. Jardin, M.S. Chance, A.M.M. Todd, and A.H. Glasser, *Nucl. Fusion* 20, 638 (1980).
- ⁹D.A. Monticello, W. Park, S.C. Jardin, M.S. Chance, R.L. Dewar, R.B. White, R.C. Grimm, J. Manickam, H.R. Strauss, J.L. Johnson, J.M. Greene, A.H. Glasser, P.K. Kaw, P.H. Rutherford, and E.J. Valeo in Plasma Physics and Controlled Nuclear Fusion Research (IAEA, Brussels, 1980) Vol. I, p. 227.

FIGURE CAPTIONS

- Fig. 1 Pressure contours at $\phi = 0$ and $\phi = \pi$. The major axis is to the left in each picture. Large $m = 2$ magnetic islands are visible.
- Fig. 2 Rotational transform κ profile along the horizontal radii at $\phi = \pi$.
- Fig. 3 Pressure contours at various ϕ angles, with $\beta_M = 10\%$. (d) is the puncture plot of magnetic fields.
- Fig. 4 Current density contours at various ϕ angles. Broken lines indicate negative values. (d) is the central conductor current.
- Fig. 5 Pressure contours show a drastic deformation of the plasma as β_M is increased to 12%.

#85T0084

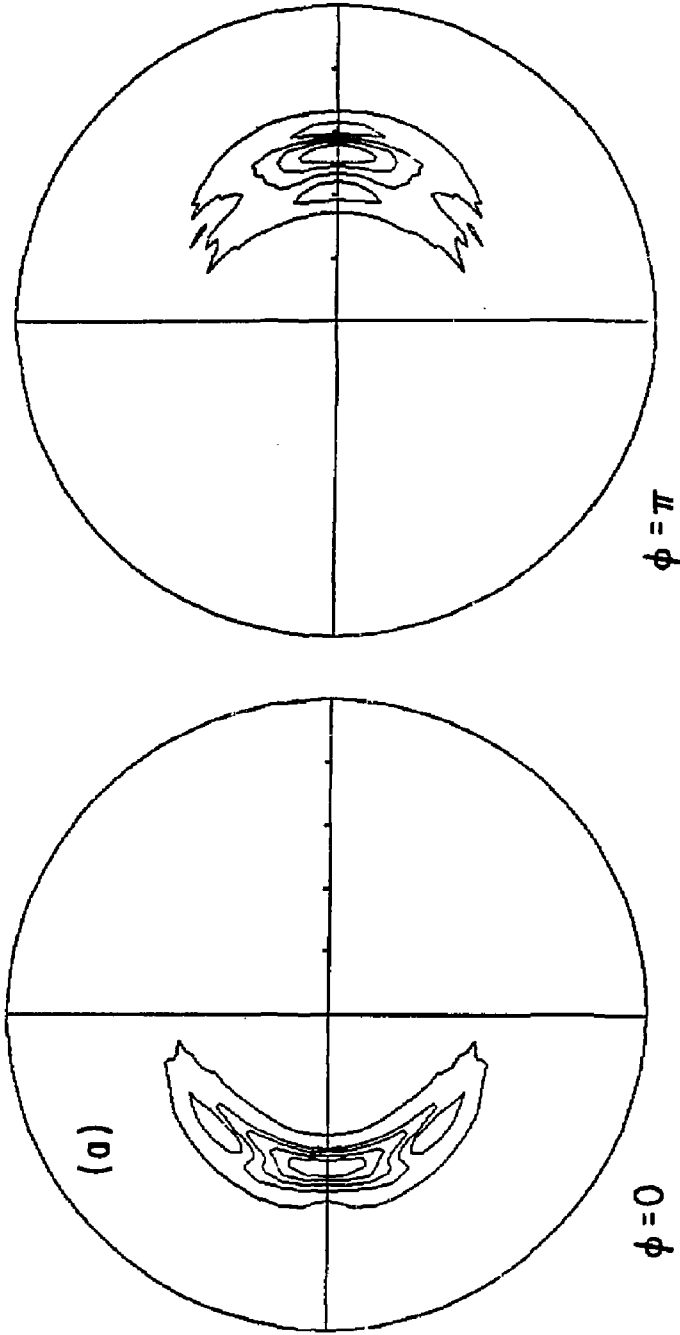


Fig. 1

#85T0085

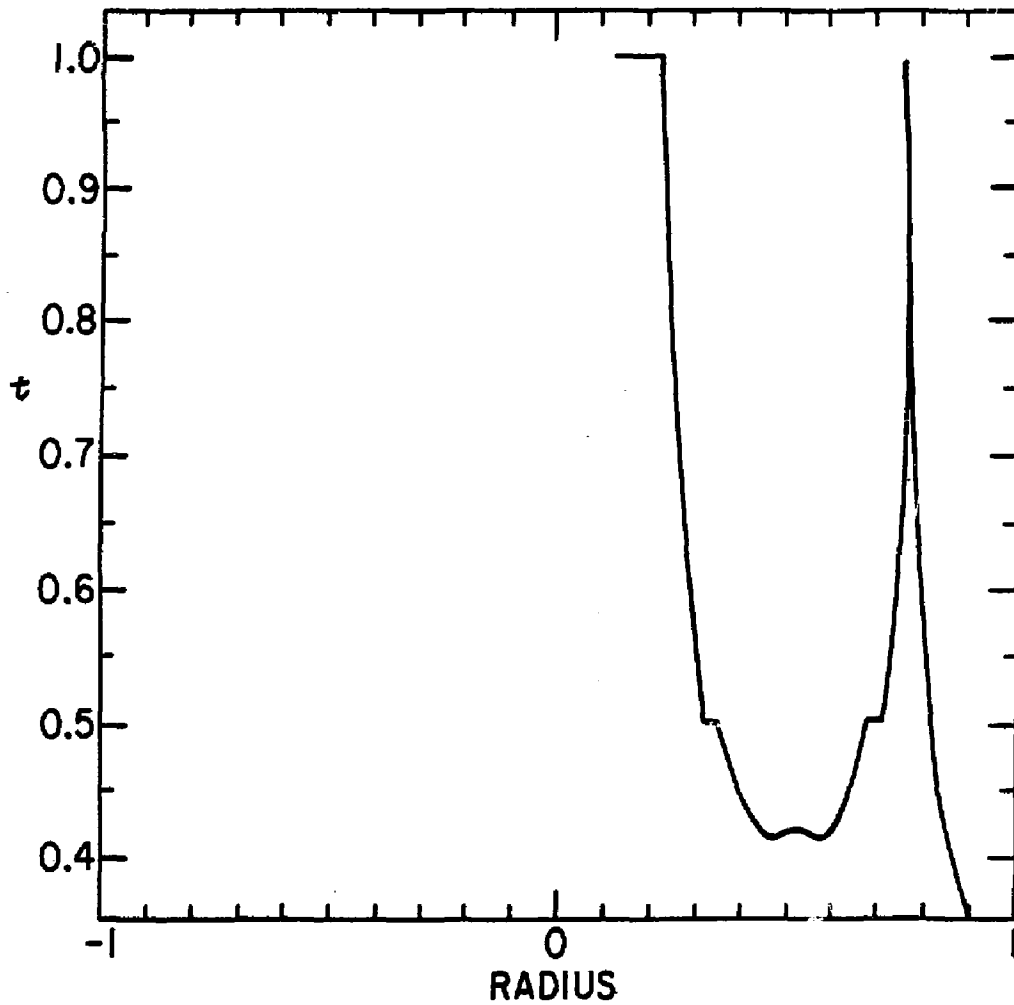


Fig. 2

85T0081

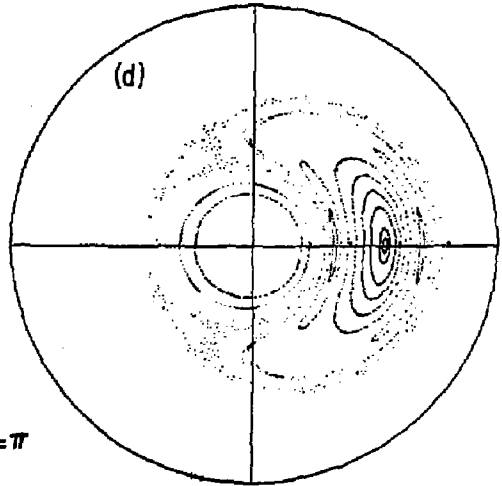
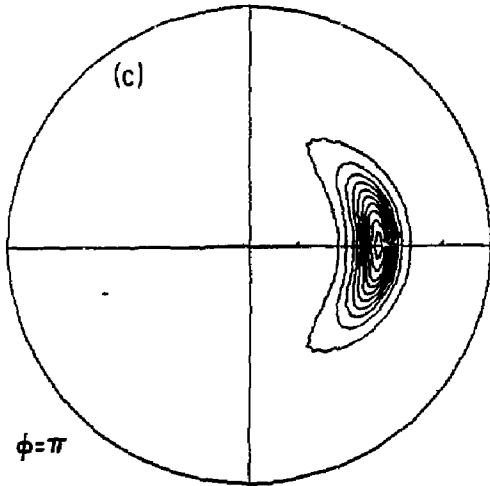
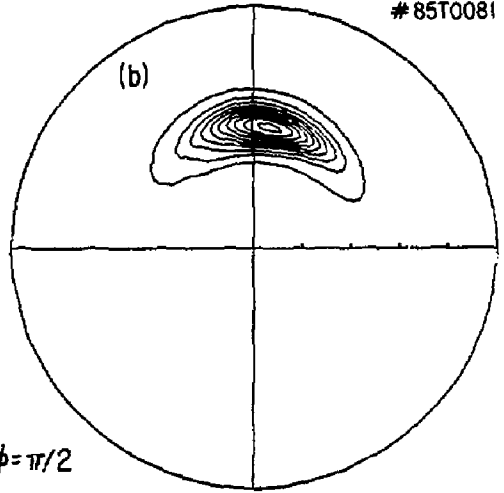
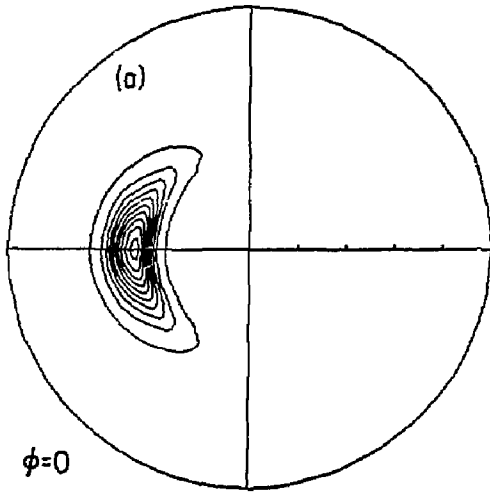


Fig. 3

#85T0083

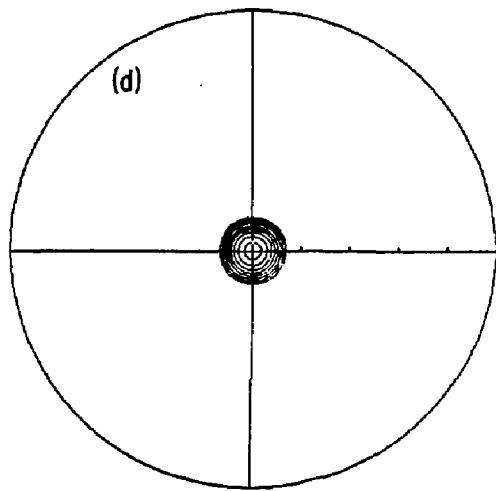
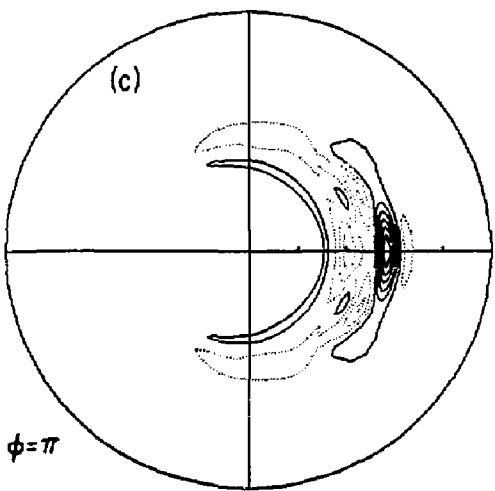
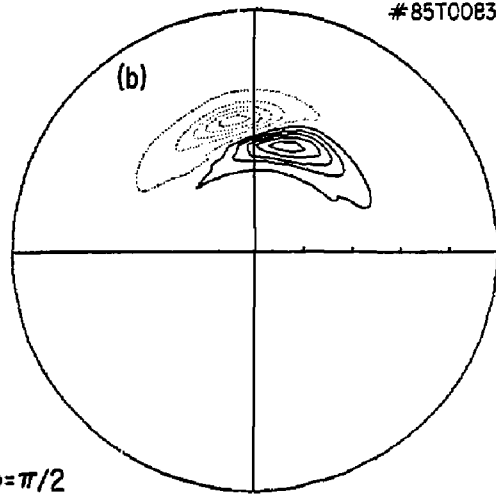
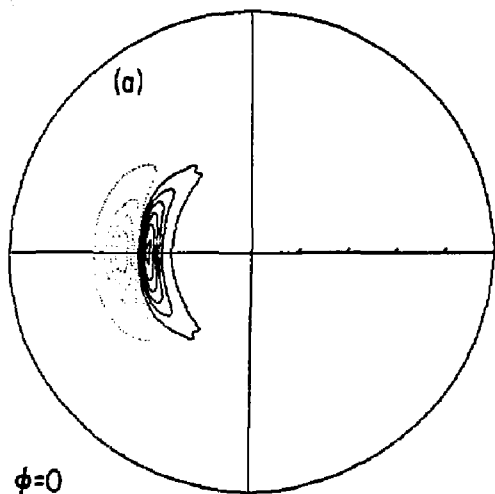
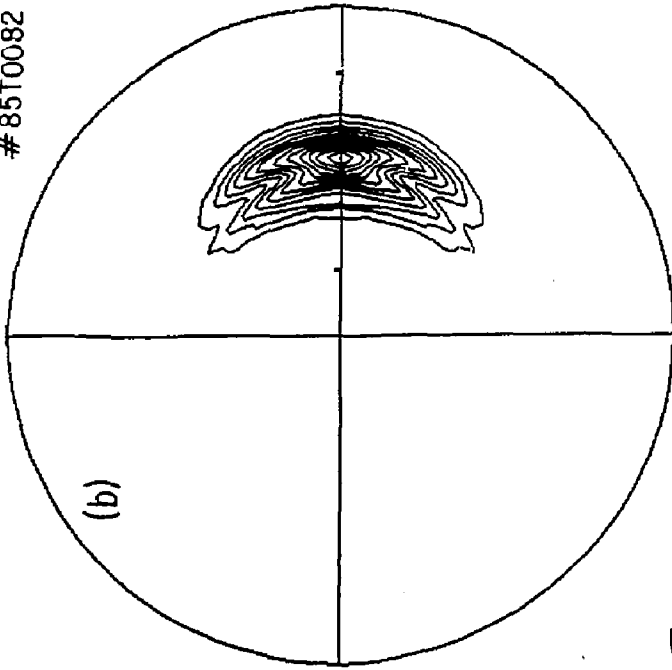
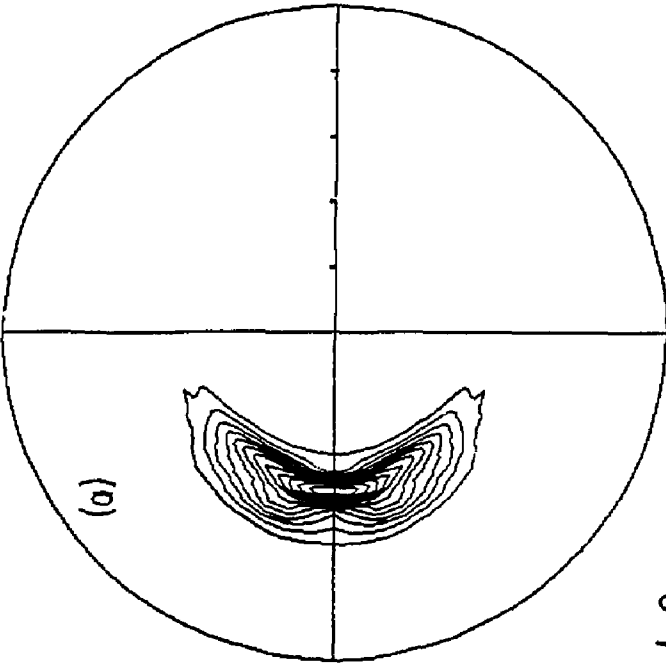


Fig. 4

#85T0082



$\phi = \pi$



$\phi = 0$

Fig. 5

EXTERNAL DISTRIBUTION IN ADDITION TO UC-20

Plasma Res Lab, Austr Nat'l Univ, AUSTRALIA
Dr. Frank J. Paoloni, Univ of Wollongong, AUSTRALIA
Prof. I.R. Jones, Flinders Univ., AUSTRALIA
Prof. M.H. Brennan, Univ Sydney, AUSTRALIA
Prof. F. Cap, Inst Theo Phys, AUSTRIA
Prof. Frank Verheest, Inst theoretische, BELGIUM
Dr. D. Palumbo, Dg XII Fusion Prog, BELGIUM
Ecole Royale Militaire, Lab de Phys Plasmas, BELGIUM
Dr. P.H. Sakaneke, Univ Estaimel, BRAZIL
Dr. C.R. James, Univ of Alberta, CANADA
Prof. J. Teichmann, Univ of Montreal, CANADA
Dr. H.M. Skarsgard, Univ of Saskatchewan, CANADA
Prof. S.R. Sreerivasan, University of Calgary, CANADA
Prof. Tudor W. Johnston, INRS-Energie, CANADA
Dr. Hannes Barnard, Univ British Columbia, CANADA
Dr. M.P. Bachynski, MFB Technologies, Inc., CANADA
Chalk River, Nucl Lab, CANADA
Zhengyu Li, SW Inst Physics, CHINA
Library, Tsing Hua University, CHINA
Librarian, Institute of Physics, CHINA
Inst Plasma Phys. Academia Sinica, CHINA
Dr. Peter Lukac, Komenskoho Univ, CZECHOSLOVAKIA
The Librarian, Culham Laboratory, ENGLAND
Prof. Schatzman, Observatoire de Nice, FRANCE
J. Radet, CEN-BEG, FRANCE
AM Dupes Library, AM Dupes Library, FRANCE
Dr. Tom Mual, Academy Bibliographic, HONG KONG
Preprint Library, Cent Res Inst Phys, HUNGARY
Dr. S.K. Trehan, Panjab University, INDIA
Dr. Indra Mohan Lal Das, Banaras Hindu Univ, INDIA
Dr. L.K. Chavda, South Gujarat Univ, INDIA
Dr. R.K. Chhajlani, Vikram Univ, INDIA
Dr. B. Dasgupta, Saha Inst, INDIA
Dr. P. Kaw, Physical Research Lab, INDIA
Dr. Phillip Rosenau, Israel Inst Tech, ISRAEL
Prof. S. Cuperman, Tel Aviv University, ISRAEL
Prof. G. Rostagni, Univ Di Padova, ITALY
Librarian, Int'l Ctr Theo Phys, ITALY
Miss Clelia De Palo, Assoc EURATOM-ENEA, ITALY
Biblioteca, del CNR EURATOM, ITALY
Dr. H. Yamato, Toshiba Res & Dev, JAPAN
Direc. Dept. Lg. Tokamak Dev. JAERI, JAPAN
Prof. Nobuyuki Inoue, University of Tokyo, JAPAN
Research Info Center, Nagoya University, JAPAN
Prof. Kyoji Nishikawa, Univ of Hiroshima, JAPAN
Prof. Sigeru Mori, JAERI, JAPAN
Library, Kyoto University, JAPAN
Prof. Ichiro Kawakami, Nihon Univ, JAPAN
Prof. Satoshi Itoh, Kyushu University, JAPAN
Dr. D.I. Chol, Adv. Inst Sci & Tech, KOREA
Tech Info Division, KAERI, KOREA
Bibliothek, Fom-Inst Voor Plasma, NETHERLANDS
Prof. B.S. Liley, University of Waikato, NEW ZEALAND
Prof. J.A.C. Cabral, Inst Superior Tech, PORTUGAL
Dr. Octavian Petrus, ALI CIJZA University, ROMANIA
Prof. M.A. Hellberg, University of Natal, SO AFRICA
Dr. Johan de Villiers, Plasma Physics, Nucor, SO AFRICA
Fusion Div. Library, JEN, SPAIN
Prof. Hans Wilhelmson, Chalmers Univ Tech, SWEDEN
Dr. Lennart Stenflo, University of UMEA, SWEDEN
Library, Royal Inst Tech, SWEDEN
Centre de Recherches, Ecole Polytech Fed, SWITZERLAND
Dr. V.T. Tolok, Kharkov Phys Tech Ins, USSR
Dr. D.D. Ryutov, Siberian Acad Sci, USSR
Dr. G.A. Eliseev, Kurchatov Institute, USSR
Dr. V.Z. Glukhikh, Inst Electro-Physical, USSR
Institute Gen. Physics, USSR
Prof. T.J.M. Boyd, Univ College N Wales, WALES
Dr. K. Schindler, Ruhr Universitat, W. GERMANY
Nuclear Res Estab, Julich Ltd, W. GERMANY
Librarian, Max-Planck Institut, W. GERMANY
Bibliothek, Inst Plasmaforschung, W. GERMANY
Prof. R.K. Janac, Inst Phys, YUGOSLAVIA